ISSN 1995-0802, Lobachevskii Journal of Mathematics, 2017, Vol. 38, No. 5, pp. 888–892. © Pleiades Publishing, Ltd., 2017.

Statistics of Freak Waves in Numerical Tank

A. I. Dyachenko[1,2*], D. I. Kachulin[1], and V. E. Zakharov[1,2,3,4]**

(Submitted by L. N. Shchur)

[1] *Novosibirsk State University, Novosibirsk-90, 630090 Russia*

[2] *Landau Institute for Theoretical Physics Russian Academy of Sciences, Chernogolovka, Moscow oblast, 142432 Russia*

[3] *Lebedev Physical Institute Russian Academy of Sciences, Moscow, 119991 Russia*

[4] *Department of Mathematics, University of Arizona, AZ, 857201, 617 N. Santa Rita, Tucson, USA*

Received September 28, 2016

Abstract—Presented are the results of experiments on calculation of Probability Distribution Functions for elevations of waters waves in numerical tank. Statistics of waves of anomalous amplitude, or freak-waves were compared both for nonlinear and linear models. Obviously, linear model demonstrates the exact Rayleigh distribution of surface elevations while PDFs for nonlinear equation have tails (for large elevations) similar to Rayleigh distribution, but with larger σ.

DOI: 10.1134/S1995080217050080

Keywords and phrases: *Nonlinear water waves, Hamiltonian formalism, modulational instability, freak waves, Zakharov equation.*

1. INTRODUCTION

The probability assessment of the ocean extreme waves appearance has important practical implications. Those peculiar object, also known as the "freak waves," are the natural part of the open seas surface wave dynamics, having linear dispersion and modulational instability as the causes of their formation. These two mechanisms are studied in the current paper for the classical 1-D water wave Hamiltonian system. Assuming moderately steep surface waves (small parameter is a steepness of the waves), the Hamiltonian can be represented by the infinite power series expansion of its natural variables. The Hamiltonian expansion up to 4th order is

$$H = \frac{1}{2}\int g\eta^2 + \psi\hat{k}\psi dx - \frac{1}{2}\int\{(\hat{k}\psi)^2 - (\psi_x)^2\}\eta dx + \frac{1}{2}\int\{\psi_{xx}\eta^2\hat{k}\psi + \psi\hat{k}(\eta\hat{k}(\eta\hat{k}\psi))\}dx. \quad (1)$$

Here $\hat{k}$ is the modulus operator ($|k|$) in Fourier space and g is the gravitational acceleration. It is well known that all of the third order terms can be excluded from the Hamiltonian (1) and the fourth order terms can be significantly simplified by using nonlinear canonical transformation $\eta(x,t), \psi(x,t) \leftrightarrow c(x,t), c^*(x,t)$. After the transformation, the Hamiltonian is drastically simplified and can be written in X-space in the compact form (for details see [1–3]):

$$H(\eta,\psi) \leftrightarrow H(c,c^*) = \int c^*\hat{V}c\,dx + \frac{1}{2}\int |c|^2\left[\frac{i}{2}(cc'^* - c^*c') - \hat{k}|c|^2\right]dx. \quad (2)$$

Here, operator $\hat{V}$ in Fourier space is so that $V_k = \omega_k/k$, $\omega_k = \sqrt{gk}$ is the dispersion law for the gravity waves on deep water.

* E-mail: alexd@itp.ac.ru

** E-mail: d.kachulin@gmail.com

2. CALCULATION OF PDFs

Hamiltonian (2) allows to obtain not only temporal Zakharov equation in compact form, but also the spatial compact equation. Temporal compact equation has the following form:

$$\frac{\partial c}{\partial t}+\hat{\Gamma}_k^p c-\hat{\Gamma}_k^d c+i\hat{\omega}_k c-i\hat{P}^+\frac{\partial}{\partial x}\left(|c|^2\frac{\partial c}{\partial x}\right)=\hat{P}^+\frac{\partial}{\partial x}(\hat{k}|c|^2 c). \tag{3}$$

Here $(\hat{P}^+)^2=\hat{P}^+=\frac{1}{2}(1-i\hat{H})$ is the projection operator to the upper half-plane (or it is step function $\theta(k)$ in k-space). The spatial compact equation has the following form:

$$\begin{aligned}\frac{\partial c}{\partial x}+\hat{\Gamma}_\omega^p c-\hat{\Gamma}_\omega^d c+\frac{i}{g}\frac{\partial^2 c}{\partial t^2}=\frac{\hat{P}^-}{2g^3}\frac{\partial^3}{\partial t^3}\left[\frac{\partial^2}{\partial t^2}\left(|c|^2 c\right)+2|c|^2\ddot{c}+\ddot{c}^* c^2\right]\\ +\frac{i\hat{P}^-}{g^3}\frac{\partial^3}{\partial t^3}\left[\frac{\partial}{\partial t}\left(c\hat{\omega}|c|^2\right)+\dot{c}\hat{\omega}|c|^2+c\hat{\omega}\left(\dot{c}c^*-c\dot{c}^*\right)\right].\end{aligned} \tag{4}$$

It solves the spatial Cauchy problem for surface gravity wave on the deep water. Initial condition at $x=0$ is provided by wavemaker. Physical variables can be recovered by canonical transformation. Calculation of PDFs must be performed in stationary turbulent state. For this reason pumping $(\hat{\Gamma}_k^p,\hat{\Gamma}_\omega^p)$ and damping $(\hat{\Gamma}_k^d,\hat{\Gamma}_\omega^d)$ were added to the temporal (3) and spatial (4) equations. Here pumping coefficients Γ_k^p, Γ_ω^p are the following:

$$\Gamma_k^p(k)=\begin{cases}\gamma_k & \text{for } |k-k_0|\le\pi\times10^{-2}\,[\mathrm{m}^{-1}],\\ 0 & \text{for } |k-k_0|>\pi\times10^{-2}\,[\mathrm{m}^{-1}],\end{cases}\quad \Gamma_\omega^p(\omega)=\begin{cases}\gamma_\omega & \text{for } |\omega-\omega_0|\le0.2\,[\mathrm{rad\ s}^{-1}],\\ 0 & \text{for } |\omega-\omega_0|>0.2\,[\mathrm{rad\ s}^{-1}],\end{cases}$$

where k_0 is the wave number of the carrier wave. Coefficient of pumping γ_k was equal to 10^{-3} $[\mathrm{s}^{-1}]$ or less, coefficient γ_ω was equal to $10^{-4}[\mathrm{m}^{-1}]$ or less.

Damping coefficient Γ_k^d was turned on, if the average value of c_k (which is c_C) in the vicinity of $k_{\max}$ was larger than roundoff errors. To clarify, the value of c_C, which is $c_C=\frac{1}{10}\sum_{i=9}^{0}|c_{k_{\max}-i}|$ controls the damping in the following way:

$$\Gamma_d(k)=\begin{cases}\alpha k^2, & \text{if } c_C \text{ is 10 times greater then roundoff errors,}\\ 0, & \text{otherwise}\end{cases}$$

with coefficient $\alpha=0.9/\tau k_{\max}^2$. The choice of α maximizes the damping and controls the integration scheme stability in the time. The damping term in spatial equation (4) was arranged similarly.

To reach the stationary turbulent state, one can start from different initial conditions. We started from the initial conditions in the form of the perturbed monochromatic wave:

$$\begin{aligned}c(x,0)&=c_0e^{ik_0x}+\sum\delta c_k e^{ikx+\phi_k}\quad\text{for temporal equation,}\\ c(0,t)&=c_0e^{-i\omega_0t}+\sum\delta c_\omega e^{-i\omega t+\phi_\omega}\quad\text{for spatial equation.}\end{aligned} \tag{5}$$

Calculations were performed in the periodic domain $x\in[0,L]$, $L=1000$ [m] for temporal equation (3) and in the periodic domain $t\in[0,T]$, $T=154$ [s] for spatial equation (4). The length of carrier wave was equal to 10 [m] ($k_0=\frac{\pi}{5}$ $[\mathrm{m}^{-1}]$), and maximal steepness $\mu\sim0.12$. Here ϕ_k and ϕ_ω are random phases. For the time-integration scheme, the 4-th order Runge–Kutta method was used. FFTW library was used for fast Fourier transformation of the nonlinear right-hand side.

The perturbation (5) causes the development of the initial condition modulational instability, which reaches the statistically homogeneous turbulent state after some time, allowiing to collect data for PDFs calculation. Starting from this time, the simulation was performed for equation (3); linear equation $i\frac{\partial c_k}{\partial t}=\omega_k c_k$ and for equation (4); linear equation $i\frac{\partial c_\omega}{\partial x}=\frac{\omega^2}{g}c_\omega$. We were interested in the $|c|$ values distribution. At the times t_n data were collected into un-normalized UPDF in the following way: $N=|c(x_i,t_n)|/\delta c$, $UPDF(N\delta c)=UPDF(N\delta c)+1$. Here δc is the discrete step for PDF. UPDF was normalized at the end of the data collection.

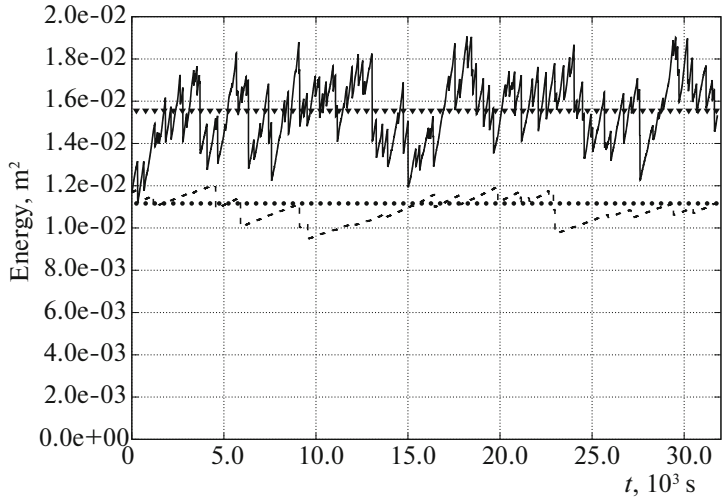

Fig. 1. Total energy dependence on time t.

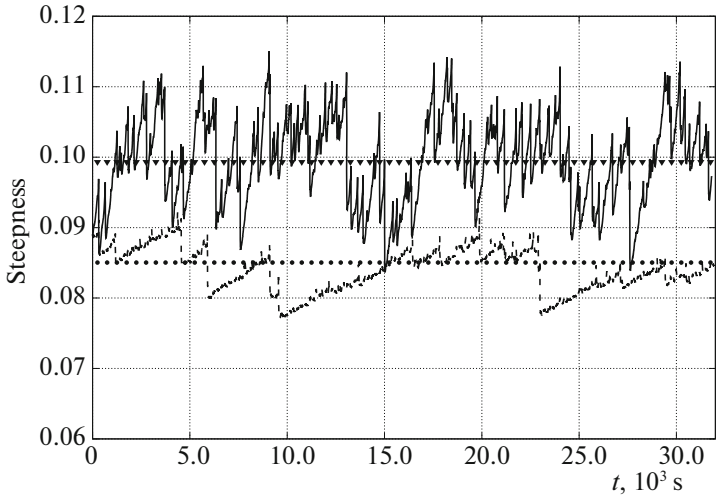

Fig. 2. Average wave steepness dependence on time t.

3. RESULTS OF PDFs CALCULATION

Figures 1, 2 show the total energy and the average wave steepness dependences on the time in the temporal equation. The solid curves on these figures correspond to the results of the numerical experiments in the nonlinear equation (3) with $\gamma_{\max} = 10^{-3}$ [s^{-1}], the dashed curves correspond to the results of the numerical experiment in the nonlinear equation (3) with $\gamma_{\max} = 10^{-4}$ [s^{-1}], the dotted lines indicate the total energy and the average steepness level in the linear equation with $\gamma_{\max} = 10^{-3}$ [s^{-1}] and $\gamma_{\max} = 10^{-4}$ [s^{-1}] respectively. Each vertical portion of the curve denotes the wave-breaking and the turning on of the dumping.

For the linear equation (i.e. the original equation with the neglected nonlinearity), one can expect normal distribution for $Re\{c(x,t)\} = r(x,t)$ and Rayleigh distribution for $|c|$:

$$PDF(r) = \frac{1}{\sigma\sqrt{2\pi}} \exp\left(-\frac{r^2}{2\sigma^2}\right), \quad PDF(|c|) = \frac{|c|}{\sigma^2} \exp\left(-\frac{|c|^2}{2\sigma^2}\right)$$

with the dispersion σ.

Figure 3 shows PDF($|c|$)/$|c|$ as the function of $|c|^2$ on logarithmic scale for numerical experiment of temporal equation with total energy level $E_{tot} \sim 1.55 \times 10^{-2}[m^2]$ and the value of average steepness

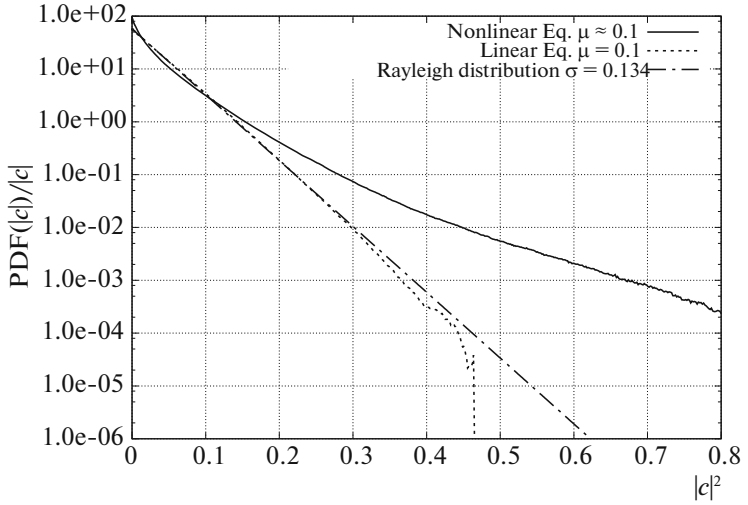

Fig. 3. PDF$(|c|)/|c|$ as the function of $|c|^2$ on logarithmic scale.

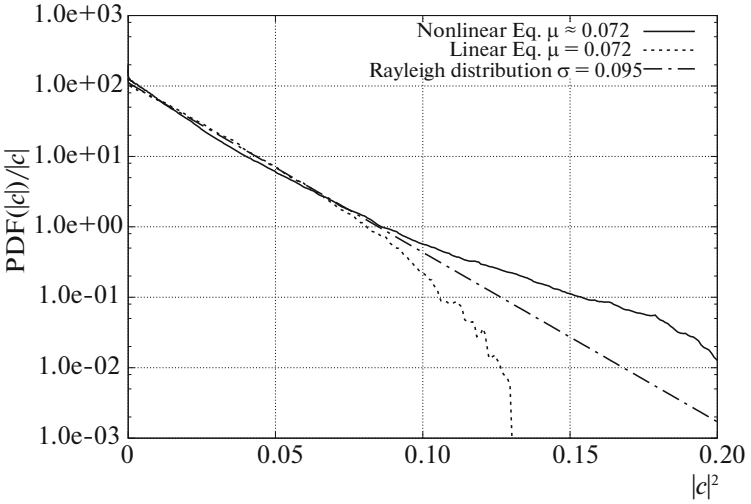

Fig. 4. PDF$(|c|)/|c|$ as the function of $|c|^2$ on logarithmic scale.

$\mu_{av} \sim 0.1$. The PDF$(|c|)/|c|$ as the function of $|c|^2$ in nonlinear equation (3) is shown by the solid curve. The dotted curve corresponds to the linear case with the same value of total energy and average steepness level. One can see that PDF in the linear case coinsides with Rayleigh distribution with dispersion $\sigma = 0.134$ (the dash dotted line on the Fig. 3). For the nonlinear equation (3) PDF is not Rayleigh, but has Rayleigh tail is the straight lines for large $|c|^2$, while the small $|c|^2$ are different. The dispersion σ of Rayleigh tail for large $|c|^2$ in the nonlinear cases obviously does depend on wave steepness (linear and nonlinear regimes coincide at small value of wave steepness) and for wave steepness $\mu \sim 0.1$ is about 2 times larger than in the linear case.

Figure 4 shows PDF$(|c|)/|c|$ as the function of $|c|^2$ in logarithmic scale for spatial equation numerical experiment with the value of average steepness $\mu_{av} \sim 0.07$. The PDF in nonlinear equation (4) is shown by the solid curve on the graph. The dotted curve corresponds to the linear case with the same value of the total energy and the average steepness level.

The normalization $(c \to \delta \cdot \sigma_{lin})$ was performed for the comparison of the PDFs for different values of the average steepness, so that for the linear equations the dispersion σ is equals to 1.

Figure 5 shows the comparison of PDF$(|\delta|)/|\delta|$ on logarithmic scale for the calculations with the different values of the average wave steepness for the linear case. One can see that the dispersion σ of

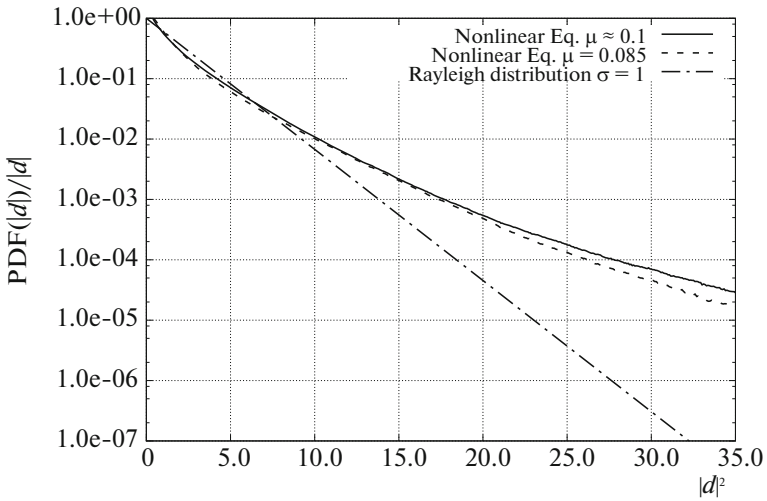

Fig. 5. Comparison of PDF($|\delta|$)/$|\delta|$ on logarithmic scale for calculations with the different values of average wave steepness.

the Rayleigh tails for large $|\delta|^2$ in the nonlinear cases slightly increases with the average total energy, and the wave steepness level increase.

So, both temporal and spatial equations (3) and (4) simulate real experiments in a flume. Thus, this pair of equations can be called as numerical tank.

ACKNOWLEDGMENTS

This work was supported by was Grant "Wave turbulence: theory, numerical simulation, experiment" no. 14-22-00174 of Russian Science Foundation. Numerical simulation was performed on the Informational Computational Center of the Novosibirsk State University.

REFERENCES

1. A. I. Dyachenko, D. I. Kachulin, and V. E. Zakharov, "About compact equations for water waves," Nat. Hazards **83**, 529–540 (2016).
2. A. I. Dyachenko, D. I. Kachulin, and V. E. Zakharov, "New compact equation for numerical simulation of freak waves on deep water," J. Phys.: Conf. Ser. **681**, 012028 (2016).
3. A. I. Dyachenko and V. E. Zakharov, "Spatial equation for water waves," JETP Lett. **103**, 181–184 (2016).